AMERICAN SOCIETY FOR MICROBIOLOGY | Journal of Bacteriology

Transcriptome Analysis of *Escherichia coli* during dGTP Starvation

Mark Itsko, Roel M. Schaaper

Genome Integrity and Structural Biology Laboratory, National Institute of Environmental Health Sciences, Research Triangle Park, North Carolina, USA

ABSTRACT

Our laboratory recently discovered that *Escherichia coli* cells starved for the DNA precursor dGTP are killed efficiently (dGTP starvation) in a manner similar to that described for thymineless death (TLD). Conditions for specific dGTP starvation can be achieved by depriving an *E. coli optA1 gpt* strain of the purine nucleotide precursor hypoxanthine (Hx). To gain insight into the mechanisms underlying dGTP starvation, we conducted genome-wide gene expression analyses of actively growing *optA1 gpt* cells subjected to hypoxanthine deprivation for increasing periods. The data show that upon Hx withdrawal, the *optA1 gpt* strain displays a diminished ability to derepress the *de novo* purine biosynthesis genes, likely due to internal guanine accumulation. The impairment in fully inducing the *purR* regulon may be a contributing factor to the lethality of dGTP starvation. At later time points, and coinciding with cell lethality, strong induction of the SOS response was observed, supporting the concept of replication stress as a final cause of death. No evidence was observed in the starved cells for the participation of other stress responses, including the *rpoS*-mediated global stress response, reinforcing the lack of feedback of replication stress to the global metabolism of the cell. The genome-wide expression data also provide direct evidence for increased genome complexity during dGTP starvation, as a markedly increased gradient was observed for expression of genes located near the replication origin relative to those located toward the replication terminus.

IMPORTANCE

Control of the supply of the building blocks (deoxynucleoside triphosphates [dNTPs]) for DNA replication is important for ensuring genome integrity and cell viability. When cells are starved specifically for one of the four dNTPs, dGTP, the process of DNA replication is disturbed in a manner that can lead to eventual death. In the present study, we investigated the transcriptional changes in the bacterium *E. coli* during dGTP starvation. The results show increasing DNA replication stress with an increased time of starvation, as evidenced by induction of the bacterial SOS system, as well as a notable lack of induction of other stress responses that could have saved the cells from cell death by slowing down cell growth.

The direct DNA precursors, deoxyribonucleoside 5′-triphosphates (dNTPs), are important determinants of the progress of DNA replication, as they affect cell cycle continuity and viability. They are also critical determinants of the accuracy of DNA replication, ultimately affecting genomic stability and the long-term fitness of populations (1–5). Many studies on the role of dNTPs have been conducted with the bacterial model *Escherichia coli*, and these studies have contributed to our understanding of DNA metabolism and other aspects of cellular physiology. Examples are the effects of dNTPs on replication fork progress (6), progress through the cell cycle (7, 8), regulation of the error-prone SOS system (9), and the bacterial mutation rate (10–12).

In an ideal system, one would like the opportunity to manipulate the dNTP levels in a controlled manner, for example, by providing the cells with specific DNA precursors, such as DNA bases or nucleosides, without affecting the levels of the NTP RNA precursors. However, because RNA and DNA precursors share many pathways for their salvage and *de novo* synthesis, such treatments lead to effects on both NTPs and dNTPs, and hence selective manipulation of dNTPs without concurrent effects on the NTPs cannot readily be achieved. Also, with enteric bacteria, there is no straightforward access for externally supplied deoxyribonucleosides because of the lack of deoxyribonucleoside kinases to convert them to the corresponding deoxyribonucleotides (13). The exception is thymidine kinase, which allows for conversion of external thymidine to thymidylate (dTMP) (13). Finally, the critical step of converting ribonucleotides to deoxyribonucleotides via the enzyme ribonucleotide reductase is subject to complex feedback regulation, which is aimed at maintaining a proper dNTP/NTP ratio as well as a proper balance among the four individual dNTPs (14). This feedback precludes arbitrary manipulation of dNTP pools through RNA precursors and also makes it difficult to manipulate a single dNTP without affecting the other dNTPs.

So far, two genetic methods have been reported for *E. coli* that allow, at least in principle, manipulation of a single DNA precursor. The first is the use of thymidylate synthase gene (*thyA*)-deficient mutants. In these strains, *de novo* dTTP synthesis is blocked at the dUMP-to-dTMP step, and dTTP availability becomes dependent on the external provision of thymine or thymidine, which are converted to dTTP by the salvage pathway. By varying the thymine level in the medium, the cellular dTTP concentration can be controlled (15). This approach led to the discovery of important phenomena, such as thymine limitation, where the supply of

Received 7 March 2016 **Accepted** 16 March 2016

Accepted manuscript posted online 21 March 2016

Citation Itsko M, Schaaper RM. 2016. Transcriptome analysis of *Escherichia coli* during dGTP starvation. J Bacteriol 198:1631–1644. doi:10.1128/JB.00218-16.

Editor: R. L. Gourse, University of Wisconsin—Madison

Address correspondence to Roel M. Schaaper, schaaper@niehs.nih.gov.

Supplemental material for this article may be found at http://dx.doi.org/10.1128/JB.00218-16.

thymine is restricted, and thymine starvation and thymineless death (TLD), where thymine is completely withheld (16). These studies have contributed significantly to the understanding of important aspects of bacterial physiology, from the bidirectionality of chromosome replication (17) to a determination of factors crucial for maintaining cell shape homeostasis (18). Importantly, the TLD phenomenon has been observed in all forms of life, including bacterial, yeast, and mammalian cells, and has provided a means to kill actively growing cells, leading to anticancer and antiviral applications. See reference 19 for an extensive review of recent advances in TLD research.

Our laboratory recently discovered a second case in *E. coli* where an individual dNTP, namely, dGTP, can be specifically manipulated (20). This was achieved by combining an increased-expression allele for a specific dGTPase, encoded by the *dgt* gene (*optA1* allele) (21), with a null mutation in the guanine salvage gene *gpt*, encoding guanine phosphoribosyltransferase (22). Increased breakdown of dGTP by the dGTPase combined with an inability to recycle the resulting deoxyguanosine and guanine back to dGTP (due to the lack of *gpt*) leads to a severe reduction in the dGTP level without affecting the other dNTPs or any of the NTPs. We termed this phenomenon dGTP starvation (20). Under these conditions, the bacterial population demonstrates a number of features similar to those of TLD, including DNA synthesis arrest, development of chromosomal complexity, SOS system induction, filamentation, and loss of viability (20).

Certain worthwhile differences between dGTP starvation and TLD have also been observed. While in TLD the withdrawal of thymine from a *thyA* strain provides an absolute block for dTTP production, hypoxanthine withdrawal from the *optA1 gpt* strain provides a severe and progressive but not complete depletion of dGTP. As a consequence, the kinetics of cell death is more gradual and can be followed experimentally over a period of several hours (20). Another distinction is that the lethal effects of dGTP starvation can be overcome by the production of extragenic suppressor mutations (to be published elsewhere), which has not been observed for TLD.

The precise sequence of metabolic events leading to cell death during dGTP starvation has not been explored. Ultimately, cell death is likely associated with the breakdown of chromosomal DNA (20) as in TLD (23, 24). Global gene expression during TLD has been studied, revealing a pronounced induction of the SOS response accompanying cell death (23). In the present study, we analyzed gene expression changes in dGTP-starved cells in response to withdrawal of hypoxanthine for extended periods. The results show profound changes in the purine metabolism genes in response to hypoxanthine withdrawal, and it is likely that these changes play a role in the starvation phenomenon via the accumulation of internal guanine. At later times, SOS induction becomes apparent, which is reflective of DNA replication stress. The results further confirm the concept of unbalanced growth, in which there is a clear lack of feedback from DNA replication stress to the rest of the cellular metabolism.

MATERIALS AND METHODS

Bacterial strains. The *E. coli* strains used in this study are listed in Table 1 and are all derivatives of strain MG1655. Genetic deficiencies were introduced by P1 transduction using P1*virA*. The *optA1* allele of *dgt* was introduced linked to the *zad-220*::Tn*10* transposon (along with the nearby *tonA* and *panD* alleles) as described earlier (25). The *gpt*::mini-Tn*10 kan* defect was transferred from strain JD20450, obtained from the National BioResource Project (NIG) of Japan (http://www.shigen.nig.ac.jp/ecoli/strain/top/top.jsp). The Δ*guaA*::*kan* allele was from the Keio collection strain JW2491-1, obtained from the *E. coli* Genetic Stock Center. The Δ*lacIZ*::*cat* allele was created by the method of Datsenko and Wanner (26), using the *cat* gene from plasmid pKD3 (26) and the following primers: 5′-GTGAAACCAGTAACGTTATACGATGTCGCAGAGTATGCCG GTGTCTCTTAgtgtaggctggagctgcttc and 5′-TTATTTTTGACACCAGAC CAACTGGTAATGGTAGCGACCGGCGCTCAGCTcatatgaatatcctccttag.

TABLE 1 *E. coli* strains used in this study

Strain	Relevant genotype[a]
NR17789G	Control
NR17789R	*optA1*
NR17794	*gpt*::*kan*
NR17793	*optA1 gpt*::*kan*
NR18056	Δ*guaA*::*kan*
NR18315	Δ*lacIZ*::*cat*
NR18314	Δ*lacIZ*::*cat optA1*
NR18169	Δ*lacIZ*::*cat gpt*::*kan*
NR18170	Δ*lacIZ*::*cat optA1 gpt*::*kan*

[a] The NR17789G control strain is MG1655 carrying the *zad-220*::Tn*10*, *tonA*, and *panD* alleles (25). All other strains are NR17789G carrying the indicated markers. See Materials and Methods for more details.

Growth conditions. The strains were grown exponentially (after initiation by a 1,000-fold dilution from overnight cultures) for ~5 generations at 37°C in Vogel-Bonner (VB) minimal medium (27) supplemented with glucose (0.4%), pantothenic acid (5 μg/ml), Casamino Acids (Becton Dickinson) (1%), and hypoxanthine (50 μg/ml). At an optical density at 630 nm (OD_{630}) of 0.1, the cultures were filtered through 47-mm-diameter polycarbonate membrane filters (0.4-μm pore size; Millipore), washed with the same medium without hypoxanthine (Hx), and then resuspended at the same cell density (OD_{630} = 0.1) in the medium without Hx, and growth was continued as before. The OD_{630} was followed closely during the next 2 h, and the cells were periodically diluted with fresh, prewarmed medium without Hx to keep the OD values between 0.1 and 0.3 (low-dilution protocol) (Table 2). Samples were taken for microarray analysis (see below) at 0, 15, 30, 45, 60, and 120 min. In a parallel procedure, the *optA1 gpt* double mutant was also monitored in a nearly identical manner, using a more highly diluted culture over a 6-h incubation period in the absence of hypoxanthine (high-dilution protocol) (Table 2). The effectiveness of the latter treatment was followed microscopically by observing the extensive cellular filamentation associated with dGTP starvation (20). The data in Fig. 1 provide an example of the inhibitory and lethal effects of the starvation treatment. For this purpose, samples were withdrawn and aliquots plated on LB plates to monitor the viable counts.

RNA isolation and transcriptomic analysis. At each time point, 15 ml of each culture was mixed with 30 ml of RNAprotect bacterial reagent (Qiagen), vortexed for 5 s, incubated for 5 min at room temperature, and centrifuged for 10 min at 5,000 × *g*. The pellet was processed using a Qiagen RNeasy Midi kit with on-column DNase digestion with Qiagen DNase. The final elution of RNA from the column was performed with 160 μl RNase-free water. Each experiment was repeated 3 times for each strain at each time point.

Microarray methodology. Gene expression analysis was conducted using Affymetrix *E. coli* Genome 430 2.0 GeneChip arrays (Affymetrix, Santa Clara, CA). Total RNA was amplified as directed in the Affymetrix prokaryotic target labeling assay protocol. One microgram of amplified biotin-labeled RNA was fragmented and hybridized to each array for 16 h at 45°C in a rotating hybridization oven, using the Affymetrix target hybridization controls and protocol. Array slides were stained with streptavidin-phycoerythrin by utilizing a double-antibody staining procedure and then were washed for antibody amplification according to a Ge-

TABLE 2 Time points and OD_{630} values employed for microarray analysis of the indicated strains[a]

Time (min)	OD_{630} (dilution factor [fold])				
	Low-dilution regimen				High-dilution regimen
	wt	*optA1* strain	*gpt* strain	*optA1 gpt* strain	*optA1 gpt* strain
0	**0.097**	**0.096**	**0.094**	**0.1**	(10)
15	**0.14**	**0.14**	**0.14**	**0.14**	
30	**0.19** (2)	**0.19** (2)	**0.21** (2)	**0.19** (2)	
45	**0.116**	**0.1**	**0.12**	**0.11**	
60	**0.163** (2)	**0.16** (2)	**0.18** (2)	**0.17** (2)	
120	**0.23**	**0.22**	**0.27**	**0.17**	**0.08** (3, 9, 25, and 50[b])
180					**0.097**
240					**0.095**
300					**0.1**
360					**0.1**

[a] The strains used in this experiment were NR17789G (wt), NR17789R (*optA1*), NR17794 (*gpt*), and NR17793 (*optA1 gpt*) (Table 1). The numbers in bold represent the OD_{630} values at which samples were taken for microarray analyses. Following sampling, cultures were diluted, where appropriate, by the indicated dilution factors (in parentheses) to maintain the desired density range. See Materials and Methods for more details on the growth conditions.
[b] For the 180-, 240-, 300-, and 360-min time points, respectively.

neChip Hybridization, Wash and Stain kit and user's manual. Arrays were scanned in an Affymetrix Scanner 3000, and data were obtained with GeneChip Command Console and Expression Console software (versions 3.2 and 1.2; AGCC), using the RMA algorithm to generate .CHP files. Preliminary analyses were performed with OmicSoft Array Studio (version 7.0) software. Statistical analysis to find differentially expressed genes was performed with Partek Genomics Suite, version 6.6 (Partek, St. Louis, MO), using analysis of variance (ANOVA) with a false discovery rate of <10% for significance of individual comparisons.

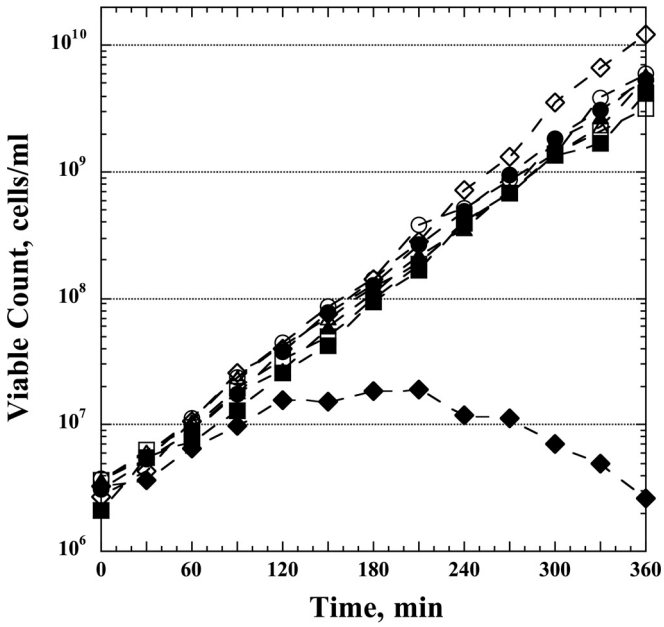

FIG 1 Loss of viability of *E. coli optA1 gpt* double mutants during dGTP starvation. Control (wt), *optA1*, *gpt*, and *optA1 gpt* strains were grown exponentially in minimal medium containing hypoxanthine (see Materials and Methods) to an OD_{630} of 0.1 and then diluted 10-fold, to an OD_{630} of 0.01, in medium with Hx (open symbols) and without Hx (closed symbols). Viability was assessed every 30 min for the next 6 h. Periodic dilutions were performed to keep the OD_{630} at 0.1 or less (50-fold dilution of all cultures at 120 min and 25-fold dilution at 270 min, except for the *optA1 gpt* strain grown without Hx). Symbols: circles, wt; squares, *optA1* strain; triangles, *gpt* strain; diamonds, *optA1 gpt* strain.

Cross-feeding assay. The cross-feeding assay used the strict guanine-requiring (Δ*guaA*) strain NR18056 (Table 1) and the four strains to be tested for guanine excretion (wild-type [wt], *optA1*, *gpt*, and *optA1 gpt* strains). The last four (NR18315, NR18315, NR18169, and NR18170) (Table 1) additionally contained a Δ*lacIZ*::*cat* chromosomal deletion. The cells were grown overnight in LB, centrifuged, and resuspended in 1× VB solution. The Δ*guaA* indicator strain was diluted 10-fold, while the tester strains were diluted 100-fold. A Chromov replicator (121 pins) was dipped into the indicator strain and used to deliver small spots on a minimal glucose plate containing pantothenic acid (5 μg/ml), Casamino Acids (1%), IPTG (isopropyl-β-D-thiogalactopyranoside; 1 mM), and X-Gal (5-bromo-4-chloro-3-indolyl-β-D-galactopyranoside; 40 μg/ml). After the spots had dried, 1.5 μl of diluted tester strain was applied manually to each previously deposited spot. The plate was incubated for 18 h at 37°C and inspected for hydrolysis of X-Gal (green or blue spots). The latter signals growth of the *lac*-proficient Δ*guaA* strain by any guanine produced by the superimposed tester strains.

Amino acid dropout experiment. VB medium agar mixtures with 0.4% glucose, 5 μg/ml pantothenic acid, and different synthetic mixtures of amino acids (each at 20 μg/ml) were poured into the wells of a 96-well plate and solidified. The amino acid mixtures contained either all 20 amino acids or 19 amino acids (one amino acid omitted). Other additions for some of the wells were hypoxanthine (50 μg/ml) and thiamine (1 μg/ml). The medium also contained IPTG (1 mM) and X-Gal (40 μg/ml) for easier visualization of bacterial growth (all strains used for the experiment contained an intact *lacZ* operon). Overnight cultures of the *optA1 gpt* and control strains were serially diluted in 10-fold steps with 1× VB buffer, and 10 μl of diluted cells was added to each well for overnight incubation at 42°C.

Microarray data accession number. Raw data and array information have been submitted to the GEO database under accession number GSE80002.

RESULTS AND DISCUSSION

Gene expression analysis during dGTP starvation. The data in Fig. 1 show the typical outcome of a dGTP starvation experiment, in which the strains initially grown in the presence of hypoxanthine were transferred to fresh medium lacking hypoxanthine (0-min time point). It can be seen that the three control strains (wt, *optA1*, and *gpt* strains) continued to grow exponentially in the new medium for the duration of the experiment, but the *optA1 gpt* double mutant clearly suffered. Its growth slowed down after the first hour, followed by a period of stalled growth, and after the 3-h

TABLE 3 Genes up- or downregulated after 120 min of hypoxanthine withdrawal[a]

Gene[b]	Function or pathway	Fold change in:			
		Control	*optA1* strain	*gpt* strain	*optA1 gpt* strain
Upregulated genes					
***purT*_b1849**	Purine *de novo* synthesis	16.3	14.3	7.6	3.4
***xanP*_b3654**	Xanthine transport	8.7	8.5	5.4	3.9
***purD*_b4005**	Purine *de novo* synthesis	8.2	8.2	4.5	4.2
***purL*_b2557**	Purine *de novo* synthesis	7.7	7.8	5.0	3.1
***cvpA*_b2313**	Colicin V production	7.6	7.3	4.4	2.8
***purM*_b2499**	Purine *de novo* synthesis	7.0	7.7	4.3	2.8
***purC*_b2476**	Purine *de novo* synthesis	6.4	5.7	4.5	2.5
***purE*_b0523**	Purine *de novo* synthesis	6.2	6.1	3.4	2.1
***purH*_b4006**	Purine *de novo* synthesis	5.9	6.6	4.0	3.3
***purK*_b0522**	Purine *de novo* synthesis	5.5	5.6	3.5	2.2
***purF*_b2312**	Purine *de novo* synthesis	4.8	5.3	3.3	2.2
***purN*_b2500**	Purine *de novo* synthesis	4.6	5.4	2.8	2.0
***codB*_b0336**	Cytosine catabolism	3.7	3.6	2.4	0.7
***codA*_b0337**	Cytosine catabolism	3.3	3.4	2.2	0.9
***gcvP*_b2903**	Glycine catabolism	2.9	3.0	2.2	1.3
***gcvT*_b2905**	Glycine catabolism	2.8	3.1	2.2	1.3
*yfdV*_b2372	Transport	2.7	2.5	1.7	1.0
***gcvH*_b2904**	Glycine catabolism	2.7	2.7	2.2	1.4
*ydeO*_b1499	Low-pH adaptation	2.5	2.9	2.0	1.5
*ydiJ*_b1687	Not known	2.4	2.6	2.1	1.1
***tsx*_b0411**	Deo/nucleoside transport	2.3	2.1	2.1	1.3
***glyA*_b2551**	One-carbon metabolism	2.3	2.1	1.7	1.3
*yfdE*_b2371	Low-pH adaptation	2.2	1.5	1.4	0.7
*menI*_b1686	Biosynthesis of menaquinone	2.2	2.1	1.9	1.1
*oxc*_b2373	Low-pH adaptation	2.2	1.6	1.7	1.6
*yfdX*_b2375	Low-pH adaptation	2.1	1.8	1.6	1.5
***purB*_b1131**	Purine *de novo* synthesis	2.1	2.1	1.7	1.5
***purR*_b1658**	Purine *de novo* synthesis	2.1	1.8	1.8	1.2
*rspB*_b1580	Not known	2.0	1.5	1.2	1.0
Downregulated genes					
*add*_b1623	Purine salvage	−3.3	−2.8	−2.9	−1.4
*ydhC*_b1660	Not known	−2.5	−2.4	−1.7	−0.8
*kdtA*_b3633	Lipopolysaccharide (LPS) biosynthesis	−2.4	−1.7	−1.6	−1.0
*yaaX*_b0005	Not known	−2.0	−1.8	−1.3	−1.3

[a] The strains used are described in Table 1 and were subjected to the low-dilution protocol. The genes listed are all those that showed an effect of at least 2-fold in the control strain.
[b] Genes shown in bold belong to the *purR* regulon.

time point the strain underwent filamentation and cell death (also see reference 20).

We previously showed that a critical parameter for observing cell death is maintenance of cells with an active growth status. Sufficiently active growth can be achieved by periodically diluting the culture such that the OD stays below 0.2. At slightly higher densities, cells are able to overcome the strictures imposed by the starvation and survive. We have proposed that death by dGTP starvation results from an imbalance between the rate of new initiations of DNA replication at the chromosomal oriC origin, which is largely determined by the nutritional status of the cells, and the ability to complete such new replication rounds, which is limited by the availability of sufficient DNA precursors. Continued initiations without the ability to complete the replication rounds leads to high origin/terminus (ori/ter) ratios, high chromosome complexity, and, ultimately, chromosomal breakdown (23, 24). Within this model, a lowering of the initiation rate at higher cell densities provides one obvious way to escape death.

The present study was aimed at understanding the metabolic changes in dGTP-starved cells. To do so, we designed two experiments. The first experiment was aimed at investigating the transcriptional consequences of loss of the Hx purine source in each of the four strains (wt, *optA1*, *gpt*, and *optA1 gpt* strains). In this experiment, hypoxanthine was withdrawn from actively growing cells starting at an OD of 0.1, and periodic 2-fold dilutions were applied to keep the OD of the growing cultures below or only slightly above 0.20 (Table 2, low-dilution regimen). Samples were taken for microarray analysis at 15, 30, 45, 60, and 120 min. At each time point, RNA samples were taken and analyzed for gene expression changes by use of an Affymetrix GeneChip *E. coli* Genome 2.0 array. This experiment was conducted independently three times.

The second experiment was aimed at following the transcriptional changes in the *optA1 gpt* strain during the entire 6-h time course, including the filamentation and cell death stage. For this experiment, we used a slightly different dilution protocol (Table 2, high-dilution regimen) in which the strain was initially highly diluted ($OD_{630} = 0.01$) and then further diluted at strategic points

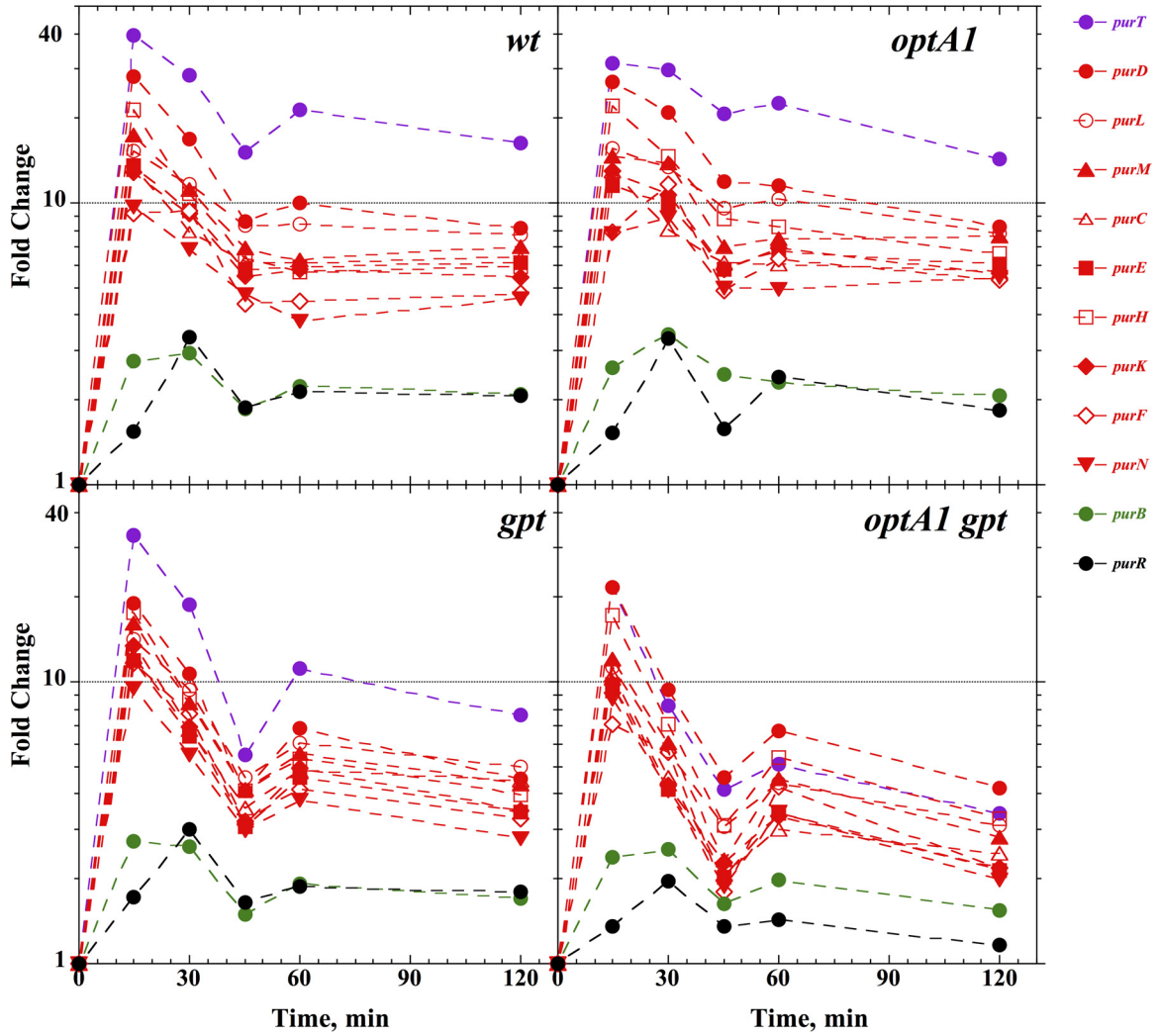

FIG 2 Induction of the various *pur* genes belonging to the *purR* regulon in control (wt), *optA1*, *gpt*, and *optA1 gpt* strains at various time points after hypoxanthine withdrawal. See the text for details.

to prevent the OD from rising above 0.1. These conditions optimize the cell death phenomenon as seen in Fig. 1. This experiment was also conducted independently three times.

Derepression of *de novo* purine synthesis upon hypoxanthine withdrawal. Withdrawal of the purine precursor hypoxanthine is expected to lead to derepression of the genes required for *de novo* purine biosynthesis, i.e., a group of genes and operons controlled by the purine repressor (PurR) (28). The microarray results confirmed this prediction (Table 3). In the wild-type strain, 33 genes were significantly affected by hypoxanthine withdrawal (29 were upregulated and 4 downregulated at a significant [2-fold] expression level). Of the 29 upregulated genes, 21 (72%) belonged to the *purR* regulon, with 16 comprising the most affected genes. Table 3 lists the 33 affected genes at the 120-min time point, while the panels of Fig. 2 and 3 show time-dependent responses for each of the four strains. Figure 2 shows a strong spike of *purR* regulon expression at the 15-min point, representing a 10- to 40-fold increase, followed by stabilization at a slightly lower level. The *purB* gene and the *purR* gene itself followed the same pattern, though at a lower level. The data in Fig. 2 further show that the pattern for the *optA1* strain was similar to that for the wt, that the response in the *gpt* strain was only marginally lower, and that the response in the *optA1 gpt* strain was significantly lower. Thus, while after 120 min the average *pur* gene was upregulated approximately 8-fold in the wt, this was reduced to about 3-fold in the *optA1 gpt* double mutant strain. This reduced ability of the strain to fully upregulate *de novo* purine synthesis may be one contributing factor to its poor ability to adapt to Hx withdrawal. A likely explanation involves the accumulation of guanine in the strain (see below).

Figure 3 presents data on two other groups of genes affected by hypoxanthine withdrawal. One group is represented by the *glyA*, *gcvP*, *gcvT*, and *gcvH* genes, which are involved in the production of glycine and its subsequent cleavage to produce one-carbon residues for the biosynthesis of several important compounds, including purines (29, 30). This group of genes is also under the control of the *purR* repressor (28), and the behavior of these genes is similar to that of the *pur* genes (Fig. 3). Interestingly, the *codAB* genes, encoding a cytosine deaminase and a cytosine (NCS1) transporter (31), respectively, while also under the control of

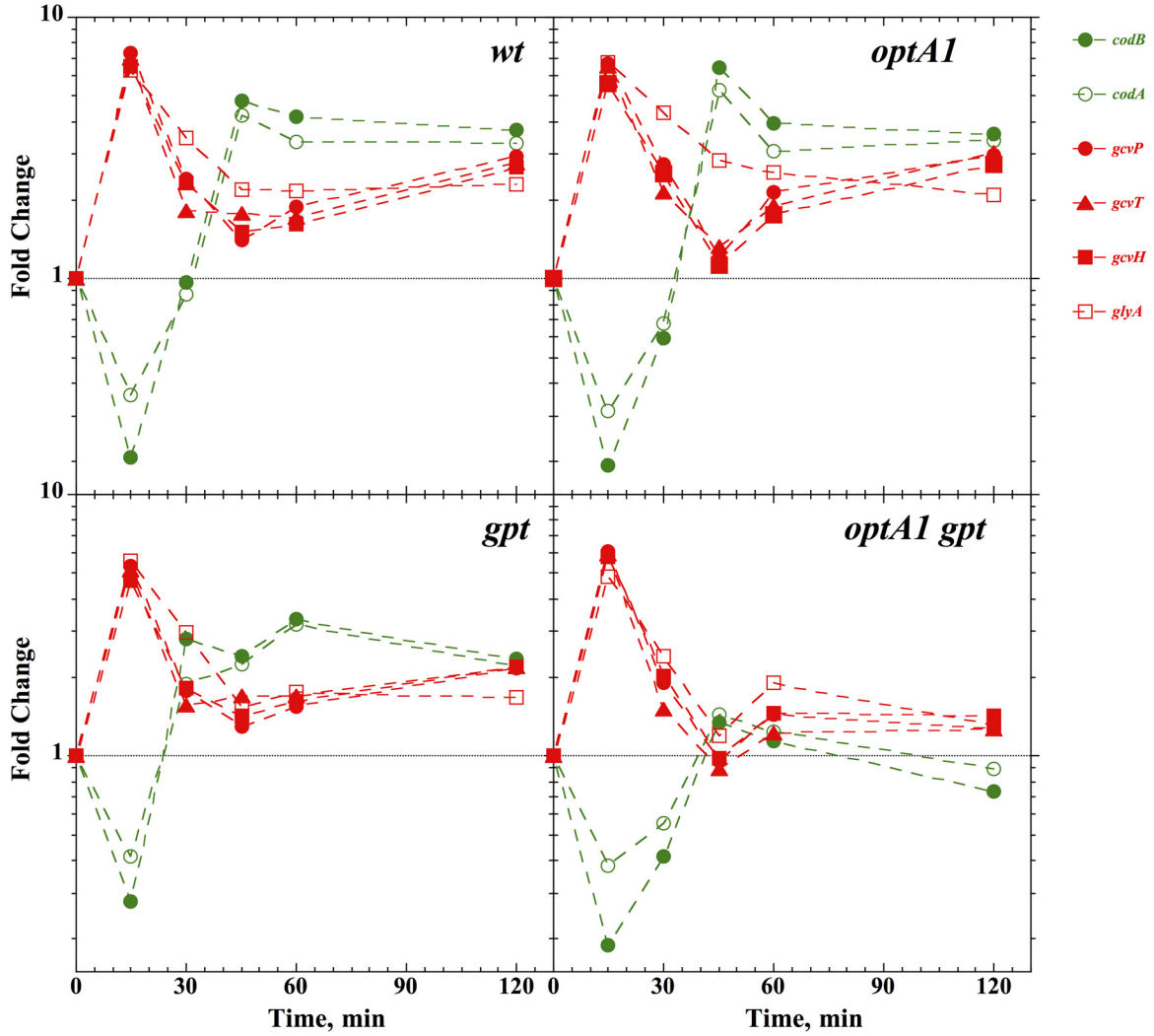

FIG 3 Induction of the *codAB*, *gcvTHP*, and *glyA* genes belonging to the *purR* regulon in control (wt), *optA1*, *gpt*, and *optA1 gpt* strains at various time points after hypoxanthine withdrawal. See the text for details.

PurR, showed the opposite response. They were depressed at the early time point (15 min) but then recovered to an elevated level similar to those of the other *pur* genes (Fig. 3). One reason may be that the *codAB* operon is additionally regulated by the NAC nitrogen-dependent regulator (32).

Guanine accumulation and excretion in the *optA1 gpt* strain. The hydrolysis of dGTP by the Dgt dGTPase produces deoxyguanosine (G-dRib), which can be converted to guanine by the DeoD purine nucleoside phosphorylase (Fig. 4). In the *optA1 gpt* strain, due to the inactive state of the *gpt* gene, encoding guanine phosphoribosyltransferase, this guanine cannot be recycled to GMP, leading to its accumulation. Because the PurR repressor uses hypoxanthine or guanine as a corepressor (33), this accumulation of guanine provides a likely explanation for the reduced derepression of the *purR*-controlled genes in the *optA1 gpt* strain. For example, Meng and Nygaard (33) showed repression of the PurR-regulated *purE* and *purD* genes by addition of guanine or hypoxanthine to an *E. coli gpt* mutant (33), while the two purine bases strongly promoted PurR binding to DNA *in vitro*, as measured by gel shift assay (33).

To test for the internal generation of guanine and its excretion, we performed a cross-feeding experiment (Fig. 5). The assay used the four donor strains (wt, *optA1*, *gpt*, and *optA1 gpt* strains), which were each grown with a recipient strain that was *guaA* deficient. GuaA-deficient strains are guanine-specific auxotrophs (34). Figure 5 shows that only the *optA1 gpt* strain produced enough guanine to sustain growth of the Δ*guaA* strain, as evidenced by its hydrolysis of X-Gal (green areas). This result is consistent with high levels of guanine accumulation in the *optA1 gpt* strain. Since guanine serves as a corepressor of PurR, this provides a plausible rationale for the observed reduced ability of the strain to derepress the regulon.

It should be noted that in the absence of the *gpt* gene product (Gpt), guanine can alternatively be converted to GMP by the *hpt* gene product (Hpt [hypoxanthine phosphoribosyltransferase]) (35). The Hpt affinity ($1/K_m$) and turnover (k_{cat}) for guanine are 20- and 6-fold lower, respectively, than those of Gpt (35), thus making the enzyme nearly 200-fold less active for guanine usage. Nevertheless, Hpt activity is likely responsible for at least some conversion of excess guanine to GMP (36). This source of GMP

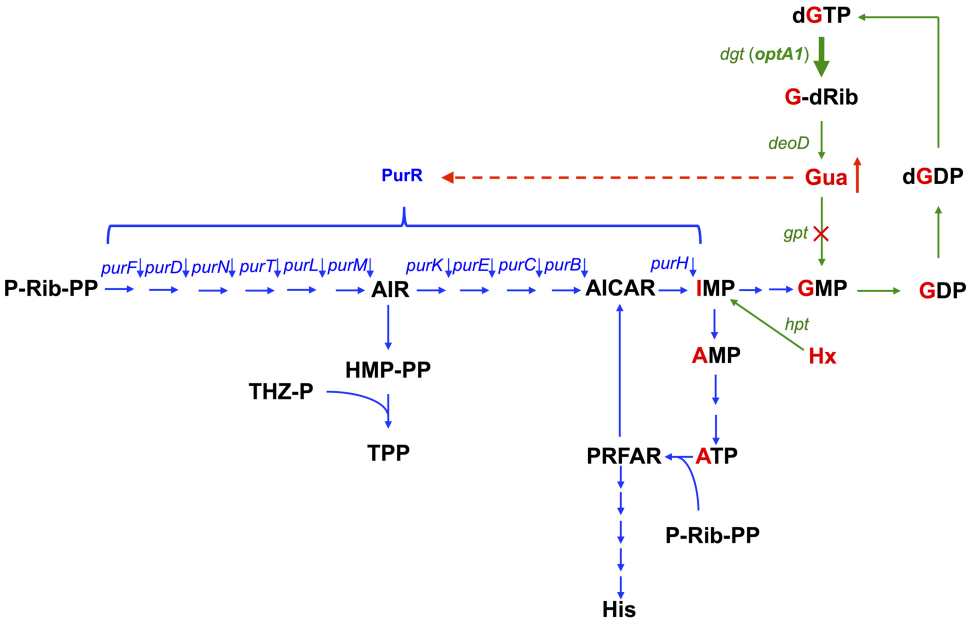

FIG 4 Flow diagram of metabolic intermediates in purine biosynthesis. Green arrows indicate the enzymatic steps for turnover of the guanine moiety (labeled in red) within the guanine nucleotide pools, with the thick arrow indicating the elevated levels of dGTP triphosphohydrolase (*dgt* up-promoter allele in the *optA1* strain). Also indicated in green is the Hpt-mediated salvage of hypoxanthine (Hx) to yield IMP. The blue arrows represent the mainstream *de novo* purine biosynthesis pathway, as well as its interconnections with histidine biosynthesis (from ATP and P-Rib-PP), resulting in AICAR production, and with thiamine biosynthesis (TPP) from the intermediate AIR. The red dashed line indicates the repressive effect of accumulated guanine (Gua) on the PurR-controlled genes (in the *optA1 gpt* strain). *dgt*, dGTP triphosphohydrolase gene; *deoD*, purine nucleoside phosphorylase gene; *gpt*, guanine phosphoribosyltransferase gene; *hpt*, hypoxanthine phosphoribosyltransferase gene; *purR*, purine repressor gene (encodes the transcription factor controlling *de novo* synthesis of purine nucleotides); Gua, guanine; Hx, hypoxanthine; G-dRib, deoxyguanosine; P-Rib-PP, 5′-phosphoribosyl-1-pyrophosphate (PRPP); AIR, 5′-aminoimidazole ribonucleotide; THZ-P, 4-methyl-5(β-hydroxyethyl)thiazol phosphate; HM-PP, 4-amino-5-hydroxymethyl-2-methylpyrimidine pyrophosphate; TPP, thiamine pyrophosphate; AICAR, 5-aminoimidazole-4-carboxamide ribonucleotide; PRFAR, phosphoribosyl formimino-5 aminoimidazol-4-carboxamide; His, histidine. The red cross indicates the lack of Gpt activity in the *gpt* deletion strain.

may be an explanation for the less stringent nature of dGTP starvation than that of dTTP starvation in TLD.

Gene expression changes during the lethal phase of dGTP starvation. To investigate the gene expression changes during the lethal stages of the dGTP starvation process, we used a slightly modified dilution protocol (Table 2, high-dilution regimen) in which the cells were initially diluted more deeply, such that they would reach OD values of around 0.1 at the time of harvest. Under these conditions, the strongest filamentation and cell death could be detected (Fig. 1) (20). The microarray data indicated that at the 6-h time point, 114 genes were significantly affected by a factor of 3-fold or more, with 66 genes upregulated and 48 genes downregulated, compared to the 0-h point. The results for a main subset of these affected genes (genes affected by 3.3-fold or more) are displayed in the heat maps of Fig. 6 and 7 for the up- and downregulated genes, respectively. Quantitative fold changes for each of the affected genes are provided in Tables 4 and 5. Among the induced genes, a most prominent part is played by genes belonging to the SOS regulon, such as *umuDC* (encoding the error-prone DNA polymerase Pol V), *recA*, *sulA*, *recN*, *dinD*, etc., and their appearance is fully consistent with the replication stress occurring under these conditions (20). SOS induction under the conditions of this regimen were already observed at the 120-min time point and increased steadily over the next several hours (see Fig. S1 in the supplemental material), reflecting accumulating levels of DNA distress over time.

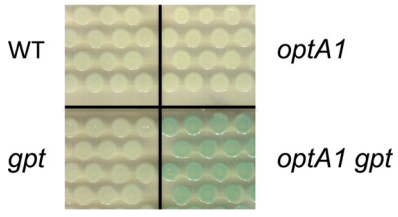

FIG 5 Cross-feeding assay demonstrating guanine excretion by the *optA1 gpt* strain under dGTP starvation conditions. In this assay, growth of a guanine-requiring (Δ*guaA*) indicator strain—as evidenced by increased X-Gal hydrolysis—is enabled by simultaneous growth with the *optA1 gpt* strain. See the text for details.

Another notable feature of dGTP starvation is upregulation of the *nrdA* and *nrdB* genes (3- to 4-fold) (Table 4). These genes encode the enzyme ribonucleotide reductase (RNR), which is responsible for the nucleoside diphosphate (NDP)-to-dNDP conversion critical for dNTP synthesis. Upregulation of *nrdAB* has been reported in the case of DNA damage (37, 38), and upregulation of dNTP depletion has been reported for the RNR inhibitor hydroxyurea (39). Thus, this effect, which is SOS independent, clearly reflects a sensing mechanism for depletion of one or more dNTPs, possibly mediated by the NrdR repressor (40).

Upregulation was also observed for a number of genes belonging to three different defective lambdoid phages present in the MG1655 genome: e14 (41), DLP-12 (42), and Qin (43). The genes of phage e14 were most notably induced, representing 10 of the 66 upregulated genes (Fig. 6; Table 4), and they were previously

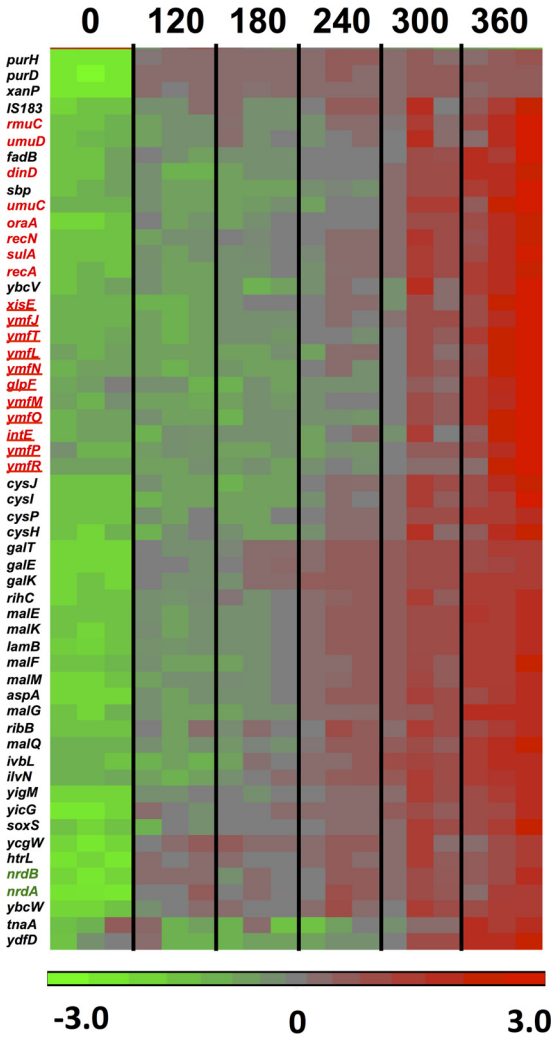

FIG 6 Heat diagram and time course for 55 genes upregulated (3.3-fold or more) in the *optA1 gpt* strain during the lethal phase of dGTP starvation. The boxes represent the results for the three replicate samples at each point. See the text for more details. The colors of the heat diagram represent the gradient of normalized expression (base 2 logarithm). Genes highlighted in red belong to the SOS regulon, with those representing the phage e14 genes underlined. The genes encoding ribonucleotide reductase subunits are shown in green.

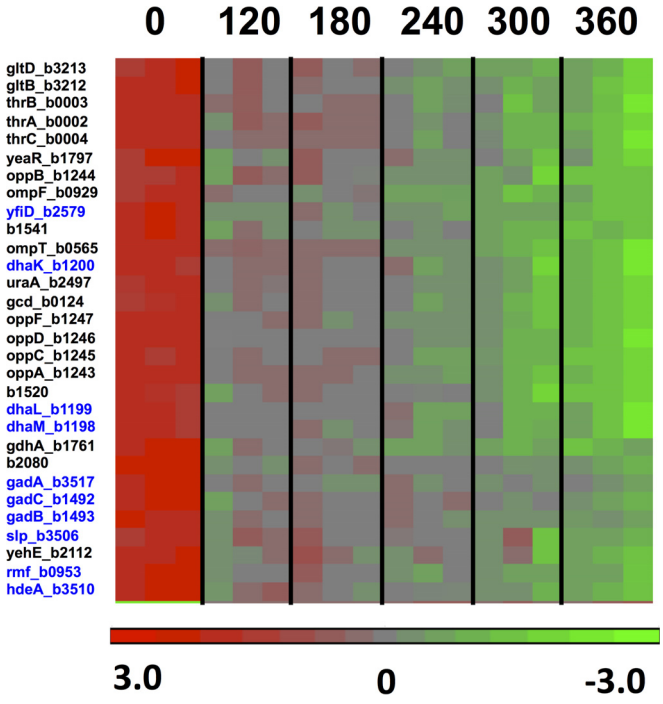

FIG 7 Heat diagram and time course for 30 genes downregulated (3.3-fold or more) in the *optA1 gpt* strain during the lethal phase of dGTP starvation. The boxes represent the results for the three replicate samples at each point. See the text for more details. Genes highlighted in blue are *rpoS*-controlled genes, which are generally induced in the stationary phase of bacterial growth or as a part of adaptation to low pH.

shown to be induced as part of the SOS response (44). Complete excision of e14 from the bacterial chromosome under SOS conditions has also been reported (41). Thus, cryptic prophage activation is another indication of the replication stress associated with dGTP starvation. As far as we know, inducibility of the DLP-12 or Qin prophage genes under stress conditions has not yet been reported in the literature.

We also noted the activation of a number of transport systems, most notably the maltose and maltodextrin transport/utilization system (45): the *malEFGKM/lamB* genes, encoding the maltodextrin ABC uptake system, were increased 8- to 33-fold, while *malQ*, encoding the enzyme amylomaltase, was induced 3.4-fold (Table 4). The maltose/maltodextrin system is under the control of the MalT transcriptional regulator, which becomes active in the presence of the trisaccharide maltotriose (45). It is possible that the filamentation and cell death in dGTP-starved cultures release maltodextrins into the medium. Alternatively, maltotriose can be generated from endogenous sources, such as glycogen (46) or trehalose (47), or by factors associated with the accumulation of unphosphorylated glucose (48). For example, during unbalanced growth, the flow of carbon in and out of the glycogen reservoir may be altered, leading to upregulated maltotriose levels, as could be the upregulation of trehalose import (*treB*; 3.1-fold) (Table 4).

Another affected system was the sulfate transport/utilization system, including the genes for the CysP/Sbp-CysUWA sulfate ABC importer (3.0- to 5.9-fold increases) (Table 4) and the CysJIH sulfite reductase (5.3- to 9.9-fold increases) (Table 4). Sulfate uptake and L-cysteine synthesis are under positive control of the CysB transcriptional regulator and the cysteine precursor (*N*/*O*)-acetyl-L-cysteine (49). Upregulation generally occurs under conditions of sulfide or cysteine limitation (49), and this may suggest the existence of some sulfide or cysteine limitation in starving cells. On the other hand, cysteine is provided in the medium as part of the Casamino Acids supplementation, which makes this possibility less likely. In an experiment described below, we noted that the presence or absence of cysteine did not affect cell death during dGTP starvation.

Downregulated genes during dGTP starvation. Among the downregulated genes in the dGTP-starved cells (Table 5), there was a large set of genes associated with growth adaptation to low pH or organic acid accumulation (*gadA*/*gadB*/*gadC* [50, 51], *ybaS* [52], *hdeA* [53], *slp* [54], *yfiD* [55, 56], and *dhaKLM* [57]). However, it is likely more relevant that most or all of these genes are also under the control of the RpoS general stress response regula-

TABLE 4 Genes upregulated 3-fold or more after 6 h of dGTP starvation in the *optA1 gpt* strain[a]

Upregulated gene	Function or pathway	Fold increase
*malK*_b4035*	Transport	33.2
*lamB*_b4036*	Transport	27.4
*malM*_b4037*	Transport	20.3
*malE*_b4034*	Transport	20.1
***ymfJ*_b1144**	e14 prophage	18.3
***ymfT*_b1146**	e14 prophage	13.5
***ymfM*_b1148**	e14 prophage	13.0
*malF*_b4033*	Transport	11.9
*cysH*_b2762	Sulfate reduction	9.9
***ymfN*_b1149**	e14 prophage	8.9
*malG*_b4032*	Transport	8.5
*sbp*_b3917	Sulfate transport	8.5
***ymfO*_b1151**	e14 prophage	7.9
***ymfL*_b1147**	e14 prophage	7.6
***sulA*_b0958**	SOS response	7.5
***recN*_b2616**	SOS response	7.5
*aspA*_b4139	Anaerobic respiration	7.4
*ilvN*_b3670	Branched-chain amino acids	7.3
*purD*_b4005	Pur regulon	7.1
***umuD*_b1183**	SOS response	6.8
*cysJ*_b2764	Sulfite reductase	6.7
***xisE*_b1141**	e14 prophage	6.6
*xanP*_b3654	Pur regulon	6.5
***rmuC*_b3832**	SOS response	6.4
*ycgW*_b1160	Proteolysis inhibition	6.2
*purH*_b4006	Pur regulon	5.9
*cysP*_b2425	Sulfate transport	5.9
***intE*_b1140**	e14 prophage	5.7
***oraA*_b2698**	SOS response	5.7
*galT*_b0758	Galactose catabolism	5.5
*ribB*_b3041	Riboflavin biosynthesis	5.4
*cysI*_b2763	Sulfite reductase	5.3
***dinD*_b3645**	SOS response	5.3
*galE*_b0759	Galactose catabolism	5.3
*yigM*_b3827	Not known	5.3
***umuC*_b1184**	SOS response	4.9
*galK*_b0757	Galactose catabolism	4.5
*ydfD*_b1576	Qin prophage	4.1
*tnaA*_b3708	Indole production (signal)	4.0
*ybcV*_b0558	DLP12 prophage	4.0
*soxS*_b4062	Oxidative stress	4.0
*ybcW*_b0559	DLP12 prophage	3.9
*yicG*_b3646	Not known	3.7
*nrdB*_b2235	Ribonucleotide reductase	3.7
*ivbL*_b3672	Branched-chain amino acids	3.7
*glpF*_b3927	Glycerol transport	3.7
*fadB*_b3846	Riboflavin biosynthesis	3.6
***ymfP*_b1152**	e14 prophage	3.6
*htrL*_b3618	LPS biosynthesis	3.5
***ymfR*_b1150**	e14 prophage	3.5
***recA*_b2699**	SOS response	3.5
*malQ*_b3416*	Transport	3.4
*rihC*_b0030	Ribonucleoside hydrolase	3.4
*nrdA*_b2234	Ribonucleotide reductase	3.4
*gadY*_b4452	Regulatory RNA	3.3
*cysU*_b2424	Sulfate transporter	3.3
*mnmE*_b3706	tRNA modification	3.2
*cpxP*_b3914	Stress response	3.2
*purM*_b2499	Pur regulon	3.1
*yiaD*_b3552	Not known	3.1
*treB*_b4240	Trehalose transport	3.1
*purL*_b2557	Pur regulon	3.1
*ryhB*_b4451	Regulatory RNA	3.1
*cysA*_b2422	Sulfate transport	3.0
*cysW*_b2423	Sulfate transport	3.0
*ryiA*_b4456	Regulatory RNA	3.0

[a] Genes shown in bold are those involved in the SOS response, and underlined genes belong to the e14 prophage. Double underlining indicates genes functioning in nucleotide metabolism. *, maltodextrin transport/utilization genes.

tor and are strongly activated upon entrance into stationary phase (58, 59). Other members of the RpoS regulon that were similarly depressed upon dGTP starvation included *otsA*, *ybaS*, *katE*, *dps*, and *rmf* (Fig. 8A; Table 5). In Fig. 8A, we plotted the gradual decline of these genes during the starvation period. Importantly, *rpoS* expression itself also declined about 1.5-fold during this period (Fig. 8A). Thus, while the cells clearly suffered from replication stress, the general stress response was not activated and was in fact depressed. It appears that under favorable growth conditions (low cell density in enriched medium), the cells persisted in a very active metabolic mode, without consideration of chromosomal distress. Likewise, in Fig. 8B, we plotted a similar decline of the Lrp (leucine-responsive regulatory protein) system, including the *lrp* gene itself (2-fold decline), which affects nearly three-fourths of the genes induced upon entry into stationary phase (59, 60). In contrast, the *hdeAB* and *gadABC* genes were previously observed to be induced during thymineless death (TLD) (23). However, in that study, the cell density during the treatment (thymine removal from the medium) was higher (23), and this may be an important distinction.

The downregulated genes (Table 5) also included the *oppABCDF* genes, encoding the oligopeptide ABC uptake system (61). This system allows *E. coli* to take up oligopeptides of 2 to 5 residues, serving both nutritional purposes and the effective recycling of cell wall (murein) peptides (62). The expression of the genes is under the control of the minor sigma factor σ^{28}, which is responsible for initiation of transcription of a number of genes involved in motility and flagellar synthesis (63). Possibly most relevant is that it is also negatively controlled by a small regulatory RNA encoded by the *gcvB* gene (64). This RNA is expressed as part of the glycine cleavage (Gcv) system important for the production of one-carbon units (29). Since hypoxanthine withdrawal led to a clear upregulation of the Gcv system (Fig. 2), increased production of GcvB may be one explanation for the downregulation of *oppABCDF*.

The importance of culture density in controlling lethality during dGTP starvation. Previous work (20) on dGTP starvation revealed the requirement for keeping cultures at low densities (OD_{630} of 0.15 or less). At slightly higher densities (OD_{630} of ~0.25), cultures are able to survive the treatment. We hypothesized that at higher densities, cells are already starting to lower their metabolic rate, including the rate of DNA replication initiation (20). It has been reported that *E. coli* cells growing in LB medium experience a diauxic growth shift at this density, resulting in a reduced growth rate due to depletion of the more easily metabolizable medium components (small oligopeptides) (65). In our experiments for the present study, the cells were grown in

TABLE 5 Genes downregulated 3-fold or more after 6 h of dGTP starvation in the *optA1 gpt* strain[a]

Downregulated gene	Function	Fold change
***gadB*_b1493**	Low-pH adaptation	−6.4
***gadC*_b1492**	Low-pH adaptation	−5.7
*uraA*_b2497	Uracil transport	−5.6
***dhaK*_b1200**	Dihydroxyacetone metabolism	−5.5
***dhaM*_b1198**	Dihydroxyacetone metabolism	−5.2
***dhaL*_b1199**	Dihydroxyacetone metabolism	−4.8
*gltB*_b3212	Glutamine degradation	−4.7
***rmf*_b0953**	Stress response	−4.6
*ydfZ*_b1541	Not known	−4.6
*oppF*_b1247*	Transport	−4.4
*gdhA*_b1761	Glutamate biosynthesis	−4.3
*gltD*_b3213	Glutamine degradation	−4.3
*thrA*_b0002	Threonine biosynthesis	−4.2
*oppB*_b1244*	Transport	−4.2
*thrC*_b0004	Threonine biosynthesis	−4.1
***gadA*_b3517**	Low-pH adaptation	−4.1
*oppD*_b1246*	Transport	−3.9
*thrB*_b0003	Threonine biosynthesis	−3.8
*ompF*_b0929	Transport	−3.6
***yfiD*_b2579**	Low-pH adaptation	−3.6
*yeaR*_b1797	Not known	−3.6
*gcd*_b0124	Glucose dehydrogenase	−3.5
*yegP*_b2080	Not known	−3.5
*oppC*_b1245*	Transport	−3.4
*yehE*_b2112	Not known	−3.4
*oppA*_b1243*	Transport	−3.3
*ompT*_b0565	Transport	−3.3
*yneE*_b1520	Swarming	−3.3
***hdeA*_b3510**	Low-pH adaptation	−3.3
***slp*_b3506**	Low-pH adaptation	−3.3
*caiF*_b0034	Carnitine metabolism	−3.3
*pyrD*_b0945	*De novo* pyrimidine synthesis	−3.3
*efeU*_b1016	Iron transport	−3.2
*ybgS*_b0753	Not known	−3.2
*pnuC*_b0751	Nicotinamide riboside transporter	−3.2
*serA*_b2913	Serine biosynthesis	−3.2
***otsA*_b1896**	High-osmolarity stress response	−3.2
*yebV*_b1836	Not known	−3.2
*yeeF*_b2014	Transport	−3.2
*ycdB*_b1019	Iron transport	−3.1
IS*092*_b4434	Small RNA	−3.1
*yeaQ*_b1795	Not known	−3.1
***ybaS*_b0485**	Low-pH adaptation	−3.1
***katE*_b1732**	Oxidative stress response	−3.1
*yceK*_b1050	Outer membrane	−3.1
*ycdO*_b1018	Iron transport	−3.0
*ydcX*_b1445	Not known	−3.0
***dps*_b0812**	Stress protein	−3.0

[a] Genes shown in bold are RpoS-dependent stationary-phase genes. *, *opp* genes encoding the oligopeptide transport system.

minimal medium with Casamino Acids to augment the growth rate. Nevertheless, not all amino acids are equally available in Casamino Acids preparations (66), and some may run out early, potentially lowering the growth rate. To gain possible insight into this question, we prepared a synthetic amino acid (solid) medium containing all 20 amino acids in equal concentration (20 μg/ml). As reported before, dGTP starvation can be demonstrated both in liquid media and on solid media, with minor adjustments (20). As shown in Fig. 9, the synthetic medium was equally effective at bringing about inactivation of the *optA1 gpt* strain, in a cell density-dependent manner. Some further insight was then sought by omitting individual amino acids from the mixture, one at a time. The majority of these omissions did not affect the phenomenology, suggesting that amino acid limitations may not be a main factor in these cases. The experiment showed two exceptions, however: lack of histidine or serine in the mixture allowed cells to overcome the lethality (Fig. 9). The case of histidine omission can readily be understood, as the biosynthesis of histidine, which is necessary under these conditions, produces an equimolar amount of 5-aminoimidazole-4-carboxamide ribonucleotide (AICAR), which is the direct precursor of IMP (Fig. 4). In this manner, histidine biosynthesis supports and stimulates purine biosynthesis, relieving dGTP starvation.

The avoidance of cell death in case of serine omission is interesting and deserves further investigation. It is possible that serine levels are a critical growth-determining factor under starvation conditions. It has been reported for *E. coli* that serine is the first amino acid to be depleted from Casamino Acids, by the action of

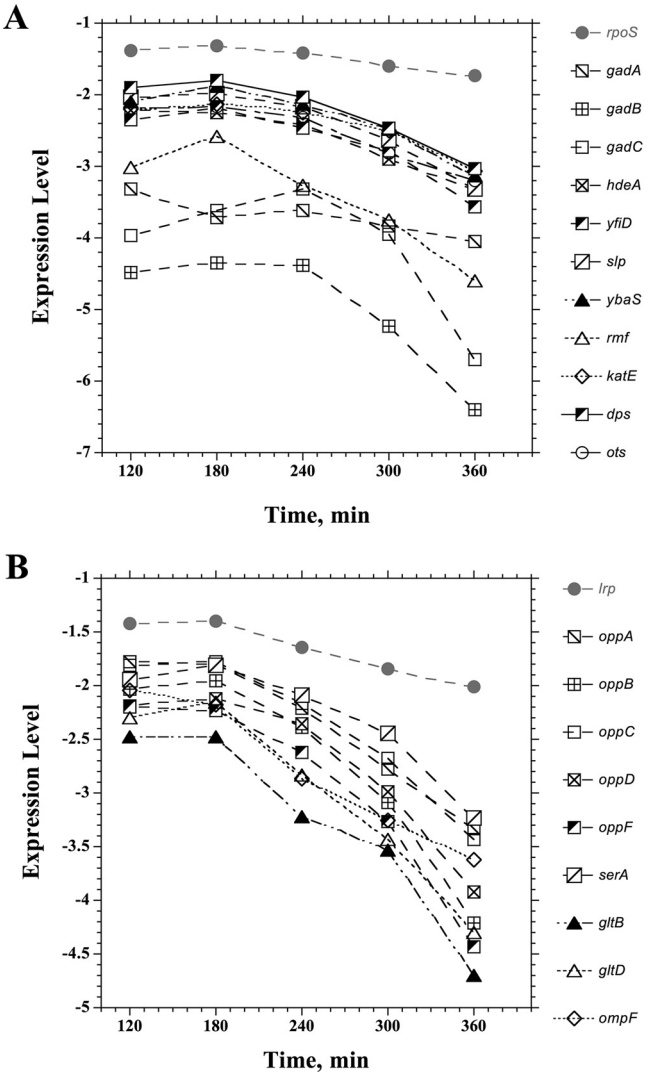

FIG 8 Decline of genes belonging to the RpoS regulon (A) or the Lrp regulon (B) during dGTP starvation. See the text for more details.

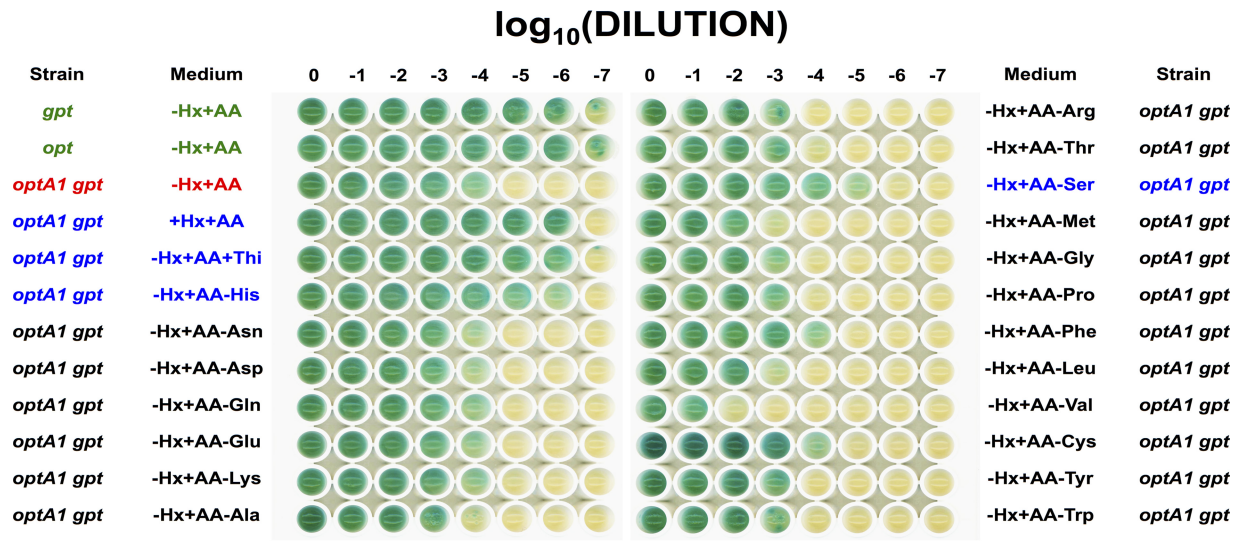

FIG 9 Growth of the indicated strains on solid media with different nutritional additions or subtractions. See Materials and Methods for more details. AA, mixture of all 20 amino acids. Omitted amino acids are indicated separately after a minus sign. The mixture without isoleucine did not support growth of any of the strains, presumably because of the toxicity of valine in the absence of isoleucine (68, 69), and the results are not shown. The first four rows represent controls. The third line (red) shows that with the synthetic mixture (−Hx+AA), the *optA1 gpt* strain was not able to grow at a low dilution. The rows in blue are the cases where growth of this strain at a low dilution was enabled by the absence of histidine (His), the absence of serine (Ser), or the addition of hypoxanthine (Hx) or thiamine (Thi). Not shown here are the +Hx−AA and −Hx−AA conditions for the *optA1 gpt* strain, which showed normal growth (no growth inhibition) (also see reference 20).

three serine deaminases (67). At the same time, the *de novo* synthesis of serine may be strained. For example, expression of *serA*, specifying the first committed step from 3-phosphoglycerate to serine (29), was downregulated >3-fold under dGTP starvation conditions (Table 5). Further, the derepression of the *purR* regulon (Fig. 2 and 3) is likely to stress serine levels by increased conversion of serine to glycine and subsequent glycine cleavage (*glyA* and *gcvTHP* genes, respectively) (Fig. 3). Under those conditions, omission of serine may lower the biomass growth rate, which in turn may protect the cell against death by dGTP starvation.

Some effects of branched-chain amino acids were also noted. Valine omission further impaired growth (Fig. 9), while isoleucine omission (not shown in Fig. 9) was toxic for all strains (see the legend to Fig. 9). These effects may not be related directly to dGTP starvation but instead to the complex regulation of branched-chain amino acids (68, 69). The slightly inhibitory effect of methionine omission may be related to the competition between methionine and purine biosynthesis pathways for one-carbon units.

Interestingly, we also noted that addition of thiamine (1 μg/ml) to the medium relieved the dGTP starvation (Fig. 9). As noted in the diagram in Fig. 4, thiamine and the purine mononucleotides are synthesized by joint pathways that diverge at the intermediate 5′-aminoimidazole ribonucleotide (AIR). It is possible that because of the repressed condition of purine *de novo* synthesis in the *optA1 gpt* strain, the drain of AIR toward thiamine pyrophosphate (TPP) further limits purine production. In the presence of thiamine, the TPP-dependent riboswitch (70) may play an important role in switching off the thiamine biosynthetic enzymes.

Increased genome complexity as revealed by microarray analysis. During dGTP starvation, ongoing replication forks slow down or stall due to the lack of dGTP, while new forks continue to be initiated at the chromosomal origin (oriC) (20). This produces increasingly complex genomes, where newly started replication forks accumulate without being able to reach the replication terminus (ter), ultimately causing DNA breakage and genome destruction (71). Interestingly, the present genome-wide expression data also provide direct evidence for this increase in genome complexity. As shown in Fig. 10, dGTP starvation in the *optA1 gpt* strain led to a marked gradient of expression ratios for genes located near the replication origin (red symbols; upregulated genes) relative to those for genes located toward the replication terminus (green symbols; downregulated genes).

In a previous paper (20), we pointed out similarities and differences between dGTP starvation and TLD (death by dTTP starvation). The differences are likely not fundamental but instead reflect the severity of the particular replication stress (abrupt and severe in TLD, due to a complete lack of dTTP, and more tempered during dGTP starvation) (20). The data in Fig. 10 bring out another, related difference, i.e., loss (breakdown) of the chromosomal origin during TLD (23, 24), while the origin region appears to be relatively stable during dGTP starvation.

Concluding comments. The present genome-wide expression data both support and inform our understanding of the metabolic changes during dGTP starvation of *E. coli*. The results reveal that a lack of derepression of *de novo* purine synthesis upon removal of the external purine source (hypoxanthine) is an important contributing factor to the starvation stress. In a parallel study (our unpublished data), we showed that mutants with suppressors of dGTP starvation capable of surviving the treatment carry defects of the PurR repressor controlling the biosynthetic *pur* regulon, consistent with this model. In addition, the data support previously proposed concepts regarding dGTP starvation (20), including production of DNA damage (i.e., induction of the SOS response), the buildup of nucleoid complexity, and the probability

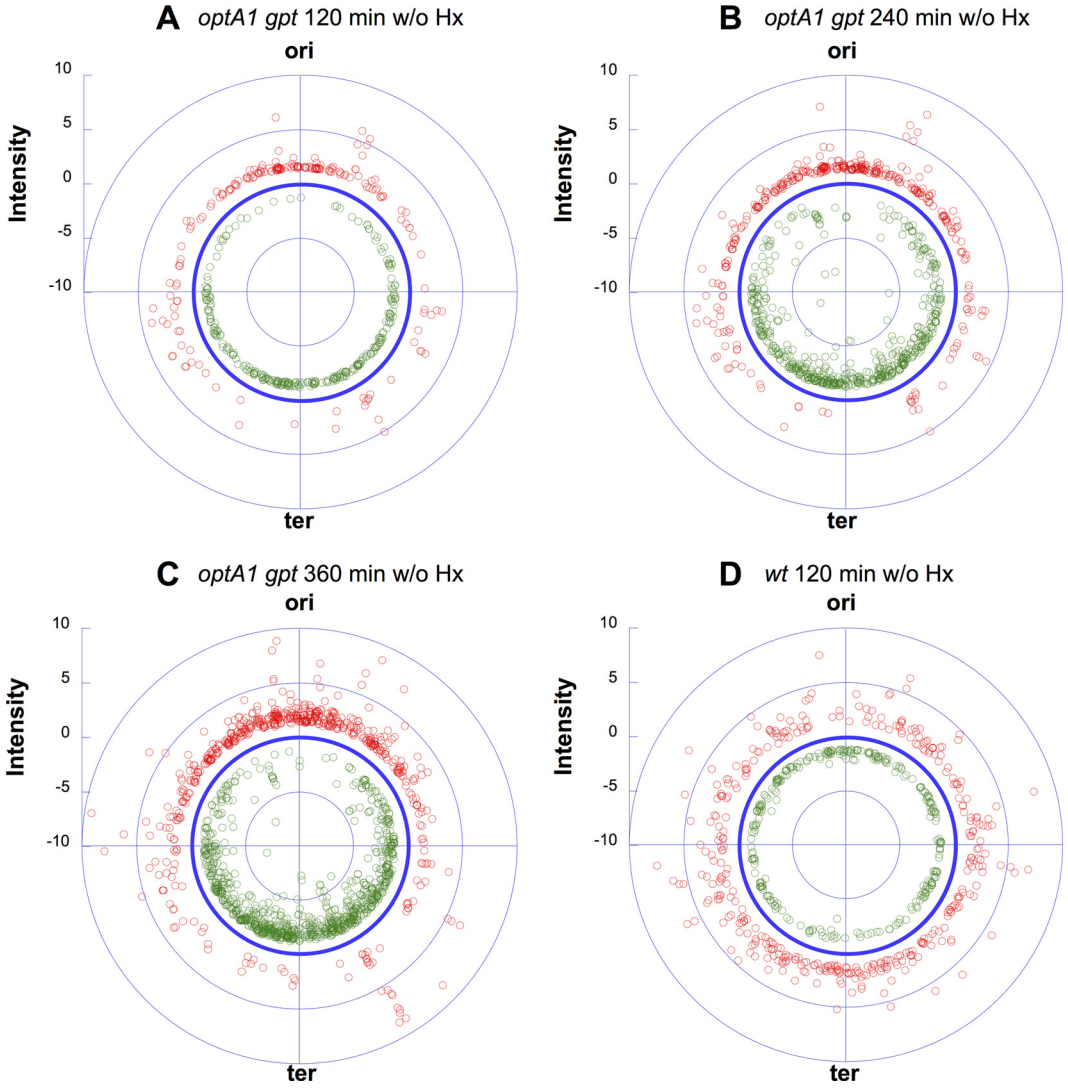

FIG 10 Diagrams showing the distributions of gene expression ratios (for significantly affected genes) along the *E. coli* chromosome in the *optA1 gpt* strain at three different time points (each relative to time zero) during dGTP starvation: 2 h (A), 4 h (B), and 6 h (C). (D) Control results for the wild-type strain cultivated without hypoxanthine for 2 h (low-dilution protocol). ori, *E. coli* replication origin (84.6 min); ter, chromosomal replication terminus (34.6 min). Red symbols indicate upregulated genes, and green symbols indicate downregulated genes, both relative to the no-effect circle (dark blue).

of escaping the lethal consequences of starvation by entering a phase of slower growth.

ACKNOWLEDGMENTS

The NIEHS Molecular Genomics Core Laboratory is acknowledged for performing the microarray analyses. We thank Natalie Itsko for providing the software code used for coordinating gene names with their map locations as provided on the EcoCyc website. We thank Deepa Singh and Thuy-Ai Nguyen of the NIEHS for their helpful review of the manuscript.

FUNDING INFORMATION

This work, including the efforts of Roel M. Schaaper, was funded by HHS | NIH | National Institute of Environmental Health Sciences (NIEHS) (ES101905).

This research was supported by project number Z01 ES101905 of the Intramural Research Program of the NIH, National Institute of Environmental Health Sciences, to Roel M. Schaaper.

REFERENCES

1. **Kunz BA, Kohalmi SE, Kunkel TA, Mathews CK, McIntosh EM, Reidy JA.** 1994. Deoxyribonucleoside triphosphate levels: a critical factor in the maintenance of genetic stability. Mutat Res **318:**1–64. http://dx.doi.org/10.1016/0165-1110(94)90006-X.
2. **Chabes A, Georgieva B, Domkin V, Zhao X, Rothstein R, Thelander L.** 2003. Survival of DNA damage in yeast directly depends on increased dNTP levels allowed by relaxed feedback inhibition of ribonucleotide reductase. Cell **112:**391–401. http://dx.doi.org/10.1016/S0092-8674(03)00075-8.
3. **Chabes A, Stillman B.** 2007. Constitutively high dNTP concentration inhibits cell cycle progression and the DNA damage checkpoint in yeast *Saccharomyces cerevisiae*. Proc Natl Acad Sci U S A **104:**1183–1188. http://dx.doi.org/10.1073/pnas.0610585104.
4. **Kumar D, Abdulovic AL, Viberg J, Nilsson AK, Kunkel TA, Chabes A.** 2011. Mechanisms of mutagenesis *in vivo* due to imbalanced dNTP pools. Nucleic Acids Res **39:**1360–1371. http://dx.doi.org/10.1093/nar/gkq829.
5. **Davidson MB, Katou Y, Keszthelyi A, Sing TL, Xia T, Ou J, Vaisica JA, Thevakumaran N, Marjavaara L, Myers CL, Chabes A, Shirahige K, Brown GW.** 2012. Endogenous DNA replication stress results in expan-

sion of dNTP pools and a mutator phenotype. EMBO J **31:**895–907. http://dx.doi.org/10.1038/emboj.2011.485.
6. **Zaritsky A, Pritchard RH.** 1971. Replication time of the chromosome in thymineless mutants of *Escherichia coli*. J Mol Biol **60:**65–74. http://dx.doi.org/10.1016/0022-2836(71)90447-5.
7. **Sun L, Fuchs JA.** 1992. *Escherichia coli* ribonucleotide reductase expression is cell cycle regulated. Mol Biol Cell **3:**1095–1105. http://dx.doi.org/10.1091/mbc.3.10.1095.
8. **Gon S, Camara JE, Klungsøyr HK, Crooke E, Skarstad K, Beckwith J.** 2006. A novel regulatory mechanism couples deoxyribonucleotide synthesis and DNA replication in *Escherichia coli*. EMBO J **25:**1137–1147. http://dx.doi.org/10.1038/sj.emboj.7600990.
9. **Maslowska KH, Makiela-Dzbenska K, Fijalkowska IJ, Schaaper RM.** 2015. Suppression of the *E. coli* SOS response by dNTP pool changes. Nucleic Acids Res **43:**4109–4120. http://dx.doi.org/10.1093/nar/gkv217.
10. **Nordman J, Wright A.** 2008. The relationship between dNTP pool levels and mutagenesis in an *Escherichia coli* NDP kinase mutant. Proc Natl Acad Sci U S A **105:**10197–10202. http://dx.doi.org/10.1073/pnas.0802816105.
11. **Ahluwalia D, Bienstock RJ, Schaaper RM.** 2012. Novel mutator mutants of *E. coli nrdAB* ribonucleotide reductase: insight into allosteric regulation and control of mutation rates. DNA Repair **5:**480–487. http://dx.doi.org/10.1016/j.dnarep.2012.02.001.
12. **Schaaper RM, Mathews CK.** 2013. Mutational consequences of dNTP pool imbalances in *E. coli*. DNA Repair **12:**73–79. http://dx.doi.org/10.1016/j.dnarep.2012.10.011.
13. **Neuhard J, Kelln RA.** 1996. Biosynthesis and conversion of pyrimidines, p 580–599. *In* Neidhardt FC, Curtiss R, III, Ingraham JL, Lin ECC, Low KB, Magasanik B, Reznikoff WS, Riley M, Schaechter M, Umbarger HE (ed), *Escherichia coli* and *Salmonella*: cellular and molecular biology, 2nd ed. ASM Press, Washington, DC.
14. **Hofer A, Crona M, Logan DT, Sjöberg BM.** 2012. DNA building blocks: keeping control of manufacture. Crit Rev Biochem Mol Biol **47:**50–63. http://dx.doi.org/10.3109/10409238.2011.630372.
15. **Beacham IR, Beacham K, Zaritsky A, Pritchard RH.** 1971. Intracellular thymidine triphosphate concentrations in wild type and in thymine requiring mutants of *Escherichia coli* 15 and K12. J Mol Biol **60:**75–86. http://dx.doi.org/10.1016/0022-2836(71)90448-7.
16. **Zaritsky A, Woldringh CL, Einav M, Alexeeva S.** 2006. Use of thymine limitation and thymine starvation to study bacterial physiology and cytology. J Bacteriol **188:**1667–1679. http://dx.doi.org/10.1128/JB.188.5.1667-1679.2006.
17. **Bird RE, Louarn J, Martuscelli J, Caro L.** 1972. Origin and sequence of chromosome replication in *Escherichia coli*. J Mol Biol **70:**549–566. http://dx.doi.org/10.1016/0022-2836(72)90559-1.
18. **Zaritsky A.** 2015. Cell-shape homeostasis in *Escherichia coli* is driven by growth, division, and nucleoid complexity. Biophys J **109:**178–181. http://dx.doi.org/10.1016/j.bpj.2015.06.026.
19. **Khodursky A, Guzmán EC, Hanawalt PC.** 2015. Thymineless death lives on: new insights into a classic phenomenon. Annu Rev Microbiol **69:**247–263. http://dx.doi.org/10.1146/annurev-micro-092412-155749.
20. **Itsko M, Schaaper RM.** 2014. dGTP starvation in *Escherichia coli* provides new insights into the thymineless-death phenomenon. PLoS Genet **10:**e1004310. http://dx.doi.org/10.1371/journal.pgen.1004310.
21. **Beauchamp BB, Richardson CC.** 1988. A unique deoxyguanosine triphosphatase is responsible for the *optA1* phenotype of *Escherichia coli*. Proc Natl Acad Sci U S A **85:**2563–2567. http://dx.doi.org/10.1073/pnas.85.8.2563.
22. **Deo SS, Tseng WC, Saini R, Coles RS, Athwal RS.** 1985. Purification and characterization of *Escherichia coli* xanthine-guanine phosphoribosyltransferase produced by plasmid pSV2gpt. Biochim Biophys Acta **8:**233–239.
23. **Sangurdekar DP, Hamann BL, Smirnov D, Srienc F, Hanawalt PC, Khodursky AB.** 2010. Thymineless death is associated with loss of essential genetic information from the replication origin. Mol Microbiol **75:**1455–1467. http://dx.doi.org/10.1111/j.1365-2958.2010.07072.x.
24. **Kuong KJ, Kuzminov A.** 2012. Disintegration of nascent replication bubbles during thymine starvation triggers RecA- and RecBCD-dependent replication origin destruction. J Biol Chem **287:**23958–23970. http://dx.doi.org/10.1074/jbc.M112.359687.
25. **Itsko M, Schaaper RM.** 2011. The *dgt* gene of *Escherichia coli* facilitates thymine utilization in thymine-requiring strains. Mol Microbiol **81:**1221–1232. http://dx.doi.org/10.1111/j.1365-2958.2011.07756.x.
26. **Datsenko KA, Wanner BL.** 2000. One-step inactivation of chromosomal genes in *Escherichia coli* K-12 using PCR products. Proc Natl Acad Sci U S A **97:**6640–6645. http://dx.doi.org/10.1073/pnas.120163297.
27. **Vogel HJ, Bonner DM.** 1956. Acetylornithinase of *Escherichia coli*: partial purification and some properties. J Biol Chem **218:**97–106.
28. **Cho BK, Federowicz SA, Embree M, Park YS, Kim D, Palsson BØ.** 2011. The PurR regulon in *Escherichia coli* K-12 MG1655. Nucleic Acids Res **39:**6456–6464. http://dx.doi.org/10.1093/nar/gkr307.
29. **Stauffer GV.** 2004. Regulation of serine, glycine, and one-carbon biosynthesis. EcoSal Plus 2004 http://dx.doi.org/10.1128/ecosalplus.3.6.1.2.
30. **Zalkin H, Nygaard P.** 1996. Biosynthesis of purine nucleotides, p 561–579. *In* Neidhardt FC, Curtiss R, III, Ingraham JL, Lin ECC, Low KB, Magasanik B, Reznikoff WS, Riley M, Schaechter M, Umbarger HE (ed), *Escherichia coli* and *Salmonella*: cellular and molecular biology, 2nd ed. ASM Press, Washington, DC.
31. **Danielsen S, Kilstrup M, Barilla K, Jochimsen B, Neuhard J.** 1992. Characterization of the *Escherichia coli codBA* operon encoding cytosine permease and cytosine deaminase. Mol Microbiol **6:**1335–1344. http://dx.doi.org/10.1111/j.1365-2958.1992.tb00854.x.
32. **Muse WB, Bender RA.** 1998. The *nac* (nitrogen assimilation control) gene from *Escherichia coli*. J Bacteriol **180:**1166–1173.
33. **Meng LM, Nygaard P.** 1990. Identification of hypoxanthine and guanine as the co-repressors for the purine regulon genes of *Escherichia coli*. Mol Microbiol **4:**2187–2192. http://dx.doi.org/10.1111/j.1365-2958.1990.tb00580.x.
34. **Lambden PR, Drabble WT.** 1973. The *gua* operon of *Escherichia coli* K-12: evidence for polarity from *guaB* to *guaA*. J Bacteriol **115:**992–1002.
35. **Guddat LW, Vos S, Martin JL, Keough DT, de Jersey J.** 2002. Crystal structures of free, IMP-, and GMP-bound Escherichia coli hypoxanthine phosphoribosyltransferase. Protein Sci **11:**1626–1638.
36. **Holden JA, Harriman PD, Wall JD.** 1976. *Escherichia coli* mutants deficient in guanine-xanthine phosphoribosyltransferase. J Bacteriol **126:**1141–1148.
37. **Filpula D, Fuchs JA.** 1977. Regulation of ribonucleoside diphosphate reductase synthesis in *Escherichia coli*: increased enzyme synthesis as a result of inhibition of deoxyribonucleic acid synthesis. J Bacteriol **130:**107–113.
38. **Gon S, Napolitano R, Rocha W, Coulon S, Fuchs RP.** 2011. Increase in dNTP pool size during the DNA damage response plays a key role in spontaneous and induced-mutagenesis in *Escherichia coli*. Proc Natl Acad Sci U S A **108:**19311–19316. http://dx.doi.org/10.1073/pnas.1113664108.
39. **Davies BW, Kohanski MA, Simmons LA, Winkler JA, Collins JJ, Walker GC.** 2009. Hydroxyurea induces hydroxyl radical-mediated cell death in *Escherichia coli*. Mol Cell **36:**845–860. http://dx.doi.org/10.1016/j.molcel.2009.11.024.
40. **McKethan BL, Spiro S.** 2013. Cooperative and allosterically controlled nucleotide binding regulates the DNA binding activity of NrdR. Mol Microbiol **90:**278–289. http://dx.doi.org/10.1111/mmi.12364.
41. **Greener A, Hill CW.** 1980. Identification of a novel genetic element in *Escherichia coli* K-12. J Bacteriol **144:**312–321.
42. **Lindsey DF, Mullin DA, Walker JR.** 1989. Characterization of the cryptic lambdoid prophage DLP12 of *Escherichia coli* and overlap of the DLP12 integrase gene with the tRNA gene *argU*. J Bacteriol **171:**6197–6205.
43. **Espion D, Kaiser K, Dambly-Chaudiere C.** 1983. A third defective lambdoid prophage of *Escherichia coli* K12 defined by the lambda derivative, λqin111. J Mol Biol **170:**611–633. http://dx.doi.org/10.1016/S0022-2836(83)80124-7.
44. **Courcelle J, Khodursky A, Peter B, Brown PO, Hanawalt PC.** 2001. Comparative gene expression profiles following UV exposure in wild-type and SOS-deficient *Escherichia coli*. Genetics **158:**41–64.
45. **Boos W, Shuman H.** 1998. Maltose/maltodextrin system of *Escherichia coli*: transport, metabolism, and regulation. Microbiol Mol Biol Rev **62:**204–229.
46. **Dippel R, Bergmiller T, Böhm A, Boos W.** 2005. The maltodextrin system of *Escherichia coli*: glycogen-derived endogenous induction and osmoregulation. J Bacteriol **187:**8332–8339. http://dx.doi.org/10.1128/JB.187.24.8332-8339.2005.
47. **Decker K, Gerhardt F, Boos W.** 1999. The role of the trehalose system in regulating the maltose regulon of *Escherichia coli*. Mol Microbiol **32:**777–788. http://dx.doi.org/10.1046/j.1365-2958.1999.01395.x.
48. **Lengsfeld C, Schönert S, Dippel R, Boos W.** 2009. Glucose- and glucokinase-controlled *mal* gene expression in *Escherichia coli*. J Bacteriol **191:**701–712. http://dx.doi.org/10.1128/JB.00767-08.

49. **Kredich NM.** 2008. Biosynthesis of cysteine. EcoSal Plus 2008 http://dx.doi.org/10.1128/ecosalplus.3.6.1.11.
50. **Castanie-Cornet MP, Penfound TA, Smith D, Elliott JF, Foster JW.** 1999. Control of acid resistance in *Escherichia coli*. J Bacteriol **181:**3525–3535.
51. **De Biase D, Tramonti A, Bossa F, Visca P.** 1999. The response to stationary-phase stress conditions in *Escherichia coli*: role and regulation of the glutamic acid decarboxylase system. Mol Microbiol **32:**1198–1211. http://dx.doi.org/10.1046/j.1365-2958.1999.01430.x.
52. **Lu P, Ma D, Chen Y, Guo Y, Chen GQ, Deng H, Shi Y.** 2013. L-Glutamine provides acid resistance for *Escherichia coli* through enzymatic release of ammonia. Cell Res **23:**635–644. http://dx.doi.org/10.1038/cr.2013.13.
53. **Gajiwala KS, Burley SK.** 2000. HdeA, a periplasmic protein that supports acid resistance in pathogenic enteric bacteria. J Mol Biol **295:**605–612. http://dx.doi.org/10.1006/jmbi.1999.3347.
54. **Mates AK, Sayed AK, Foster JW.** 2007. Products of the *Escherichia coli* acid fitness island attenuate metabolite stress at extremely low pH and mediate a cell density-dependent acid resistance. J Bacteriol **189:**2759–2768. http://dx.doi.org/10.1128/JB.01490-06.
55. **Wagner AF, Schultz S, Bomke J, Pils T, Lehmann WD, Knappe J.** 2001. YfiD of *Escherichia coli* and Y06I of bacteriophage T4 as autonomous glycyl radical cofactors reconstituting the catalytic center of oxygen-fragmented pyruvate formate-lyase. Biochem Biophys Res Commun **285:**456–462. http://dx.doi.org/10.1006/bbrc.2001.5186.
56. **Wyborn NR, Messenger SL, Henderson RA, Sawers G, Roberts RE, Attwood MM, Green J.** 2002. Expression of the *Escherichia coli yfiD* gene responds to intracellular pH and reduces the accumulation of acidic metabolic end products. Microbiology **148:**1015–1026. http://dx.doi.org/10.1099/00221287-148-4-1015.
57. **Maurer LM, Yohannes E, Bondurant SS, Radmacher M, Slonczewski JL.** 2005. pH regulates genes for flagellar motility, catabolism, and oxidative stress in *Escherichia coli* K-12. J Bacteriol **187:**304–319. http://dx.doi.org/10.1128/JB.187.1.304-319.2005.
58. **Vijayakumar SR, Kirchhof MG, Patten CL, Schellhorn HE.** 2004. RpoS regulated genes of *Escherichia coli* identified by random *lacZ* fusion mutagenesis. J Bacteriol **186:**8499–8507. http://dx.doi.org/10.1128/JB.186.24.8499-8507.2004.
59. **Tani TH, Khodursky A, Blumenthal RM, Brown PO, Matthews RG.** 2002. Adaptation to famine: a family of stationary-phase genes revealed by microarray analysis. Proc Natl Acad Sci U S A **99:**13471–13476. http://dx.doi.org/10.1073/pnas.212510999.
60. **Cho BK, Barrett CL, Knight EM, Park YS, Palsson BØ.** 2008. Genome-scale reconstruction of the Lrp regulatory network in *Escherichia coli*. Proc Natl Acad Sci U S A **105:**19462–19467. http://dx.doi.org/10.1073/pnas.0807227105.
61. **Hiles ID, Gallagher MP, Jamieson DJ, Higgins CF.** 1987. Molecular characterization of the oligopeptide permease of *Salmonella typhimurium*. J Mol Biol **195:**125–142. http://dx.doi.org/10.1016/0022-2836(87)90332-9.
62. **Goodell EW, Higgins CF.** 1987. Uptake of cell wall peptides by *Salmonella typhimurium* and *Escherichia coli*. J Bacteriol **169:**3861–3865.
63. **Arnosti DN, Chamberlin MJ.** 1989. Secondary sigma factor controls transcription of flagellar and chemotaxis genes in *Escherichia coli*. Proc Natl Acad Sci U S A **86:**830–834. http://dx.doi.org/10.1073/pnas.86.3.830.
64. **Urbanowski ML, Stauffer LT, Stauffer GV.** 2000. The *gcvB* gene encodes a small untranslated RNA involved in expression of the dipeptide and oligopeptide transport systems in *Escherichia coli*. Mol Microbiol **37:**856–868. http://dx.doi.org/10.1046/j.1365-2958.2000.02051.x.
65. **Sezonov G, Joseleau-Petit D, D'Ari R.** 2007. *Escherichia coli* physiology in Luria-Bertani broth. J Bacteriol **189:**8746–8749. http://dx.doi.org/10.1128/JB.01368-07.
66. **Street HE, Hughes JC, Lewis JC.** 1960. Studies on the growth of excised roots. X. Individual amino acids and acid-hydrolysed casein as nitrogen sources for the growth of excised tomato roots. New Phytol **59:**273–287.
67. **Zhang X, El-Hajj ZW, Newman E.** 2010. Deficiency in L-serine deaminase interferes with one-carbon metabolism and cell wall synthesis in *Escherichia coli* K-12. J Bacteriol **192:**5515–5525. http://dx.doi.org/10.1128/JB.00748-10.
68. **De Felice M, Squires C, Levinthal M, Guardiola J, Lamberti A, Iaccarino M.** 1977. Growth inhibition of *Escherichia coli* K-12 by L-valine: a consequence of a regulatory pattern. Mol Gen Genet **156:**1–7. http://dx.doi.org/10.1007/BF00272245.
69. **Salmon KA, Yang CR, Hatfield GW.** 2006. Biosynthesis and regulation of the branched-chain amino acids. EcoSal Plus 2006 http://dx.doi.org/10.1128/ecosalplus.3.6.1.5.
70. **Winkler W, Nahvi A, Breaker RR.** 2002. Thiamine derivatives bind messenger RNAs directly to regulate bacterial gene expression. Nature **419:**952–956. http://dx.doi.org/10.1038/nature01145.
71. **Simmons LA, Breier AM, Cozzarelli NR, Kaguni JM.** 2004. Hyperinitiation of DNA replication in *Escherichia coli* leads to replication fork collapse and inviability. Mol Microbiol **51:**349–358. http://dx.doi.org/10.1046/j.1365-2958.2003.03842.x.